Ortho-Chalcogenostannates as Ligands: Syntheses, Crystal Structures, Electronic Properties, and Magnetism of Novel Compounds Containing Ternary Anionic Substructures $[M_4(\mu_4\text{-}Se)(SnSe_4)_4]^{10-}$ (M = Mn, Zn, Cd, Hg), $^3_\infty\{[Hg_4(\mu_4\text{-}Se)(SnSe_4)_3]^{6-}\}$, or $^1_\infty\{[HgSnSe_4]^{2-}\}$

Michael K. Brandmayer,[a] Rodolphe Clérac,[b] Florian Weigend,[c] and Stefanie Dehnen*[a]

Abstract: By reaction of $K_4[SnSe_4]\cdot 1.5$-MeOH with $CdCl_2$ or $Hg(OAc)_2$ in water/methanol it was possible to prepare single crystals of four novel compounds that contain ternary anionic coordination oligomers and polymers: $[K_{10}(H_2O)_{16}(MeOH)_{0.5}][M_4(\mu_4\text{-}Se)(SnSe_4)_4]$ (**4**: M = Cd, **5**: M = Hg), $[K_6(H_2O)_3][Hg_4(\mu_4\text{-}Se)(SnSe_4)_3]\cdot MeOH$ (**6**), and $K_2[HgSnSe_4]$ (**7**), which were structurally characterized by single-crystal X-ray diffraction. The optical absorption properties of the isostructural compounds **4** and **5**, as well as those of the recently reported Zn (**2**) and Mn (**3**) analogues, were studied by UV-visible spectroscopy. These investigations showed the quaternary phases to have relatively small optical gaps for their molecular size (2.2–2.6 eV), which are similar to the excitation energies that were observed for mesostructured solids of the respective combination of elements. According to DFT investigations on the ternary anions, an experimentally observed difference between the absorption behavior of the d^{10} compounds **2**, **4**, and **5** and the open-shell d^5 compound **3** is in line with different characters of the frontier orbitals in the two cases. Both the calculations and a magnetic measurement on **3** demonstrated antiferromagnetic coupling between the μ_4-Se-bridged Mn centers.

Keywords: anions · cadmium · magnetic properties · mercury · selenostannates

Introduction

The function of binary main-group element molecules as ligands in molecular, nanosized, or mesostructured coordination compounds of transition metals has been studied with increasing intensity for several years.[1] Besides basic research that aims to develop systematic synthesis routes or to systematically combine different elements within the ternary M/E′/E subunits (M = transition metal; E′ = heavy Group 13–15 element; E = S, Se, Te), there is a distinct focus on the investigations of their physical properties. Compounds that incorporate two different types of heavy main-group elements and a transition metal are of specific interest with respect to opto-electronics or magnetism. This especially has led to investigations of systems in which E′ is a Group 14 element; here the M/E′/E elemental combination can be viewed as a combination of fragments of transition metal chalcogenide and tetrel chalcogenide extended solids that are known to possess (semi)conducting or photo-semiconducting properties.[2] The influence of the elemental combination on the opto-electronic properties seems to be very subtle; therefore, variation of M, E′, or E within known or related structures might provide series of compounds with "tunable" properties.

Ternary M/E′/E compounds that have been reported to date range from molecular species such as [Na(2,2,2-crypt)][$\{(C_5Me_5)(CO)_2MnSn)_3S_4\}$Na(THF)$_3$][3] and [$(PhSnS_3)_2$-$(CuPPhMe_2)_6$],[4] through a large number of mesostructured phases such as $Rb_3[AgGe_4Se_{10}]\cdot 2H_2O$,[5] $(CP)_3[Fe_4S_4Ge_4S_{10}]$ (CP = cetylpyridinium),[6a] and $(CP)_x[Pt_ySn_4Se_{10}]$ ($x = 1.9$–2.8, $y = 0.9$–1.6),[6b] to several solid-state phases such as $K_2[MnSnS_4]$[6c] and $Ba[Cu_6Ge_2S_8]$.[7]

Such materials can be synthesized in principle by two routes: formation of the ternary compounds from separate

[a] M. K. Brandmayer, Dr. S. Dehnen
Institut für Anorganische Chemie
Universität Karlsruhe (TH)
Engesserstr., Geb. 30.45
76128 Karlsruhe (Germany)
Fax: (+49) 721-608-7021
E-mail: dehnen@chemie.uni-karlsruhe.de

[b] Dr. R. Clérac
Centre de Recherche Paul Pascal CRPP-CNRS, UPR-8641
115, Avenue du Dr. A. Schweitzer
33600 Pessac (France)

[c] Dr. F. Weigend
Institut für Nanotechnologie
Forschungszentrum Karlsruhe GmbH
76021 Karlsruhe (Germany)

 DOI: 10.1002/chem.200400521

sources of M, E′, and E during the reaction,[3–5,6c,7] or by reaction of binary precursors.[6a,b,d] The latter additionally allows us to study the stability of the binary species under the given reaction conditions, for example, the reaction behavior of E′/E reactants in the presence of reactive transition metal complexes. Moreover, it provides the possibility to choose the size of the "spacer" between the transition metal centers, provided that the E′/E precursor, which does not necessarily represent the thermodynamically preferred E′/E species, does not decompose during the reaction. Whereas numerous investigations using this route have been successful with binary alloys or anions of Group 15/16 elements, attempts to stabilize Group 14/16 anions in the coordination sphere of transition-metal centers by the same methods leads to a completely different reaction pathway with E′–E bond cleavage.[8] Recently, modification of the synthesis method allowed the isolation of ternary or quaternary species with substructures in which transition metal centers are linked by chalcogenotetrelate anions. By reactions templated with the surfactant CP, for example, it was possible to generate the aforementioned mesostructured phases, most of which contain adamantane-type $[E'_4E_{10}]^{4-}$ ions (E′ = Sn, Ge; E = S, Se), although some contain $[Sn_2S_6]^{4-}$ or $[SnSe_4]^{4-}$ ions that bridge transition metal centers in purely inorganic, three-dimensional networks.[6] As intended, the resulting phases show uncommon electronic properties such as very narrow band gaps or intense photoluminescence, although they have not been structurally characterized until now.

We are interested in synthesizing and characterizing systems with ternary structural units by the reaction of orthoselenostannate anions $[SnSe_4]^{4-}$, the behavior of which towards transition metal compounds is still largely unknown. In the course of our investigations,[8,9] we recently isolated and structurally characterized quaternary compounds $[K_{22}(MeOH)_{17}(H_2O)_8][Co_4(\mu_4\text{-}Se)(SnSe_4)_4]$ (**1a**),[9a] $[K_{36}(\mu_6\text{-}Cl)_2(H_2O)_{11}(MeOH)_{32}][SnSe_4][Co_4(\mu_4\text{-}Se)(SnSe_4)_4]_3$ (**1b**)[9b] and $[K_{10}(H_2O)_{16}(MeOH)_{0.5}][M_4(\mu_4\text{-}Se)(SnSe_4)_4]$ (M = Zn: **2**, M = Mn: **3**),[9c] which contain the formerly unknown type of ternary selenide anion $[M_4(\mu_4\text{-}Se)(SnSe_4)_4]^{10-}$. Compounds **1–3** were obtained by reactions of $K_4[SnSe_4]$[10] or $K_4[SnSe_4]\cdot 1.5\,MeOH$[9c] with $[Co(en)_3]Cl_3$ (en = 1,2-diaminoethane), $MnCl_2\cdot 4\,H_2O$, or $ZnCl_2$ in H_2O/MeOH. In the highly charged, purely inorganic M/Sn/Se anions of **1–3**, chalcogenostannate anions were shown to function as ligands in molecular coordination compounds for the first time by single-crystal X-ray analysis. Recently, a number of solvent-free sulfur homologues $K_{10}[M_4Sn_4S_{17}]$ (M = Mn, Fe, Co, Zn) were reported; however, these were prepared by combining the elements in a K_2S flux.[11] These inorganic selenide and sulfide compounds are structural analogues of the carbosilane "scaphane" cluster $[Si_8C_{17}H_{36}]$[12] and oxides such as $Na_{10}[Be_4Si_4O_{17}]$.[13]

Suitable modification of the reaction conditions used in our previous investigations[9c] enabled the syntheses of four novel quaternary compounds with M = Cd or Hg: $[K_{10}(H_2O)_{16}(MeOH)_{0.5}][Cd_4(\mu_4\text{-}Se)(SnSe_4)_4]$ (**4**), $[K_{10}(H_2O)_{16}(MeOH)_{0.5}][Hg_4(\mu_4\text{-}Se)(SnSe_4)_4]$ (**5**), $[K_6(H_2O)_3][Hg_4(\mu_4\text{-}Se)(SnSe_4)_3]\cdot MeOH$ (**6**), and $K_2[HgSnSe_4]$ (**7**), which were structurally characterized by single-crystal X-ray diffraction. Compounds **4** and **5** are heavier homologues of **2** and also contain ternary $[M_4(\mu_4\text{-}Se)(SnSe_4)_4]^{10-}$ ions; compound **6** shows an as-yet unknown, three-dimensional ternary Hg/Sn/Se network based on fragments of the coordination oligomers in **5**; compound **7** includes a third variant of a Hg/Sn/Se substructure representing infinite Hg/Sn/Se chains within a solvent-free solid-state phase. We present here the crystal structures of **4–7** and discuss the electronic properties of the isotypic compounds **2–5**, which were investigated by UV-visible spectroscopy, quantum chemical investigations using DFT[14] methods, and magnetic measurements.

Results and Discussion

Syntheses: Scheme 1 outlines the syntheses of quaternary compounds **4–7** by reactions of $K_4[SnSe_4]\cdot 1.5\,MeOH$[9c] with $CdCl_2$ or $Hg(OAc)_2$. As with the reaction yielding the lighter homologue of **4** and **5** (i.e., compound **2**) it was found to be more appropriate to use a methanol solvate of $K_4[SnSe_4]$[10] instead of the pure ternary phase in order to optimize reaction rates and yields.

In addition to the quaternary compounds, the chalcogenodistannate salt $[K_4(MeOH)_4][Sn_2Se_6]$ crystallizes after layering with nonpolar solvents, as observed with the syntheses of **1–3**.[9] This co-product results from dimerization of $[SnSe_4]^{4-}$ ions with liberation of Se^{2-} ions [Eq. (1)], which are then available to be incorporated in the ternary substructures.

$$2\,[SnSe_4]^{4-} \rightleftharpoons [Sn_2Se_6]^{4-} + 2\,Se^{2-} \qquad (1)$$

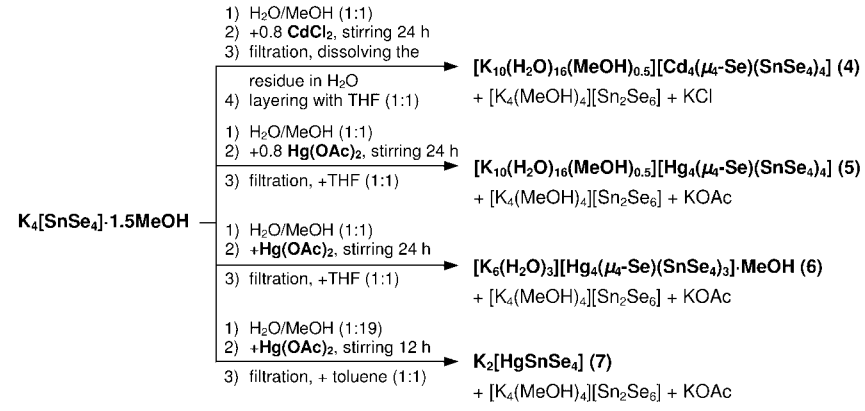

Scheme 1. Syntheses of **4–7** by reaction of $K_4[SnSe_4]\cdot 1.5\,MeOH$ with $CdCl_2$ or $Hg(OAc)_2$ in H_2O/MeOH. All compounds identified after layering are listed.

The equilibrium given in Equation (1) is known to favor the monomer side for homologous $[SnS_4]^{4-}$ ions in aqueous solution;[15] the observed shift to the right-hand side is thus forced by the generation of the ternary compounds, that is, by the formation of stable M–Se (M = Co, Mn, Zn, Cd, Hg) bonds with free Se^{2-} ions during the reactions described here.

Reactions with $Hg(OAc)_2$ differ from the others in two respects: firstly, one must remove an insoluble black precipitate of HgSe before layering, which causes lower yields; secondly, different K/Hg/Sn/Se compounds are observed upon subtle variations of stoichiometry or solvents. This indicates lower stability of the ternary Hg/Sn/Se compounds relative to the binary chalcogenide HgSe, and lower stability or solubility differences of the coordination oligomer in **5** with respect to the competing coordination polymers observed in **6** and **7**.

Formation of **5** is only observed if less than equimolar amounts of $Hg(OAc)_2$ are present, whereas equimolar amounts of the reactants lead to selective crystallization of **6**. This correlates with respective reaction schemes [Eqs. (2) and (3)], which include all identified reaction products.

$$6\,K_4[SnSe_4]\cdot 1.5\,MeOH + 5\,Hg(OAc)_2 \xrightarrow{H_2O/MeOH} [K_{10}(H_2O)_{16}(MeOH)_{0.5}][Hg_4Sn_4Se_{17}]\ (\mathbf{5}) + HgSe + [K_4(MeOH)_4][Sn_2Se_6] + 10\,KOAc \quad (2)$$

$$5\,K_4[SnSe_4]\cdot 1.5\,MeOH + 5\,Hg(OAc)_2 \xrightarrow{H_2O/MeOH} [K_6(H_2O)_3][Hg_4Sn_3Se_{13}]\cdot MeOH\ (\mathbf{6}) + HgSe + [K_4(MeOH)_4][Sn_2Se_6] + 10\,KOAc \quad (3)$$

By using a less polar H_2O/MeOH mixture (1:19) and layering with toluene afforded the solvent-free phase **7**. As with the synthesis of **5**, equimolar amounts of the reactants were used, which is again consistent with the reaction scheme [Eq. (4)]. Therefore, selective crystallization of **7** instead of either **5** or a product mixture must be attributed to the different solubilities of the possible products.

$$4\,K_4[SnSe_4]\cdot 1.5\,MeOH + 4\,Hg(OAc)_2 \xrightarrow{H_2O/MeOH} 2\,K_2[HgSnSe_4]\ (\mathbf{7}) + [K_4(MeOH)_4[Sn_2Se_6] + 2\,HgSe + 8\,KOAc \quad (4)$$

Crystal structures: Compounds **4** and **5** precipitate as yellow and orange crystals, respectively. These are obtained in good yields (70–80%) and crystallize isotypically in the tetragonal space groups $P4_12_12$ and $P4_32_12$ (the presented data were from individual crystals crystallizing in $P4_12_12$). All single crystals that were crystallographically investigated so far were essentially free of racemic twinning, as can be seen from the Flack parameters[16] (0.02(1) max). Compound **6** forms dark orange, very small cuboids. The structure was solved and refined in the rhombohedral space group $R3m$ with consideration of partial racemic twinning [Flack parameter 0.42(4)].[17] Crystals of compound **7** are ruby red, diamond-shaped, and crystallize in the tetragonal space group $I\bar{4}2m$, with partial racemic twinning [Flack parameter 0.38(9)].[17] Table 1 summarizes details of the single-crystal X-ray analyses of **4**–**7**.[16–18]

Crystal structures of 4 and 5: Since both compounds are isotypic with the recently reported **2** and **3**,[9c] the molecular structures of the Cd and Hg homologues are not discussed in detail here; we rather focus on a comparison of the series of compounds **2**–**5** and on a discussion of the crystal packing. Figure 1 shows the structure of the ternary anion

Table 1. Data of the single-crystal X-ray structural analyses of **4**–**7**.[17] The structures were solved by direct methods (SHELXS-86)[18] and were refined by full-matrix least-squares procedures on F^2 (SHELXL-97).[18]

	4	**5**	**6**	**7**
formula	$C_{0.5}H_{34}Cd_4K_{10}O_{16.5}Se_{17}Sn_4$	$C_{0.5}H_{34}Hg_4K_{10}O_{16.5}Se_{17}Sn_4$	$CH_{10}Hg_4K_6O_4Se_{13}Sn_3$	HgK_2Se_4Sn
M_r [g mol^{-1}]	2961.96	3314.72	2505.60	713.32
crystal size [mm^3]	0.20×0.20×0.16	0.12×0.12×0.10	0.09×0.09×0.09	0.14×0.10×0.10
color	yellow	orange	dark orange	red
diffractometer	STOE IPDS	STOE IPDS	STOE IPDS	STOE IPDS
radiation	$Ag_{K\alpha}$	$Mo_{K\alpha}$	$Mo_{K\alpha}$	$Ag_{K\alpha}$
λ [Å]	0.56087	0.71073	0.71073	0.56087
T [K]	203	150	203	203
crystal system	tetragonal	tetragonal	rhombohedral	Tetragonal
space group	$P4_12_12$ (No. 92)	$P4_12_12$ (No. 92)	$R3m$ (No. 160)	$I\bar{4}2m$ (No. 121)
a [10^2 pm]	15.623(2)	15.62(2)	15.125(4)	8.0681(11)
c [10^2 pm]	25.434(5)	25.440(5)	16.247(3)	6.9497(14)
V [10^6 pm^3]	6208.0(18)	6208.7(18)	3218.7(12)	452.39(13)
Z	4	4	3	2
ρ_{calcd} [g cm^{-3}]	3.169	3.546	3.878	5.237
$\mu(Mo_{K\alpha})$ $\mu(Ag_{K\alpha})$ [mm^{-1}]	7.179	22.109	27.590	19.662
2Θ range [°]	3–45	3–50	4–45	6–44
independent reflns	8227	4241	1004	247
R(int)	0.1404	0.0642	0.1477	0.1574
observed reflns [$I > 2\sigma(I)$]	6523	3658	759	225
Flack parameter[16]	0.00(3)	0.015(10)	0.42(4)	0.38(9)
parameters[17]	216	220	74	15
R_1	0.0626	0.0376	0.0739	0.0798
wR_2	0.1544	0.0712	0.1594	0.1592
max. peak/hole [e 10^{-6} pm^{-3}]	2.065/−1.572	0.905/−0.659	1.407/−2.121	2.530/−3.941

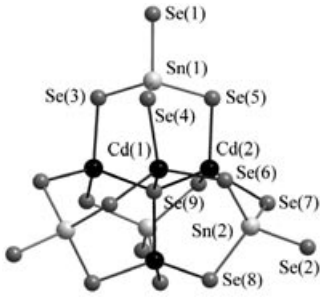

Figure 1. Structure of the ternary anion in **4**. Selected bond lengths and angles are listed and compared to those of isotypic compounds **2**, **3**, and **5** in Table 2. Formal rotations of the $[SnSe_4]^{4-}$ caps around axes Sn(1)···Se(9) or Sn(2)···Se(9), which result in chiral, C_2-symmetric molecules are 13.54(4)–20.17(3)° in **4** and 13.67(3)–18.10(4)° in **5**.

$[Cd_4Sn_4Se_{17}]^{10-}$ in **4**. A view of the crystal packing in the unit cell is given in Figure 2. Selected bond lengths and angles for the chiral, C_2-symmetric clusters and their counterion environments are listed in Table 2, together with the respective data for isotypic compounds **2** and **3**.

The M–Se bond lengths in **2**–**4** follow the trend of the ionic radii for four-coordinate M^{2+} ions,[19] when going from $M^{2+} = Zn^{2+}$ (71 pm) through Mn^{2+} (80 pm), to Cd^{2+} (91 pm). However, Cd–Se bond lengths in **4** and those of Hg–Se in **5** are nearly identical, which is not consistent with the larger ionic radius of Hg^{2+} (98 pm) but with the similar covalent radii[20] (Cd: 149 pm, Hg: 150 pm) and thus reflects an increasing covalent character of the M–Se bonds in the heavier homologues. Structural parameters within the $[SnSe_4]^{4-}$ groups are only slightly affected by the nature of the coordinated transition-metal center. Starting at nearly identical values for the Sn–Se_t and Sn–(μ-Se) bond lengths in **2**, one observes a separation by a maximum of 2.4 pm into somewhat shorter Sn–Se_t bonds and somewhat longer Sn–(μ-Se) bonds in **3**, **4**, and **5**. According to the trends in the M–Se and Sn–Se bond lengths, the volumes of the ternary anions (represented by their Se···Se edge lengths) and thus the volumes of the unit cells, which always contain four formula units, lie in the order $V(\mathbf{5}) \approx V(\mathbf{4}) > V(\mathbf{3}) > V(\mathbf{2})$.

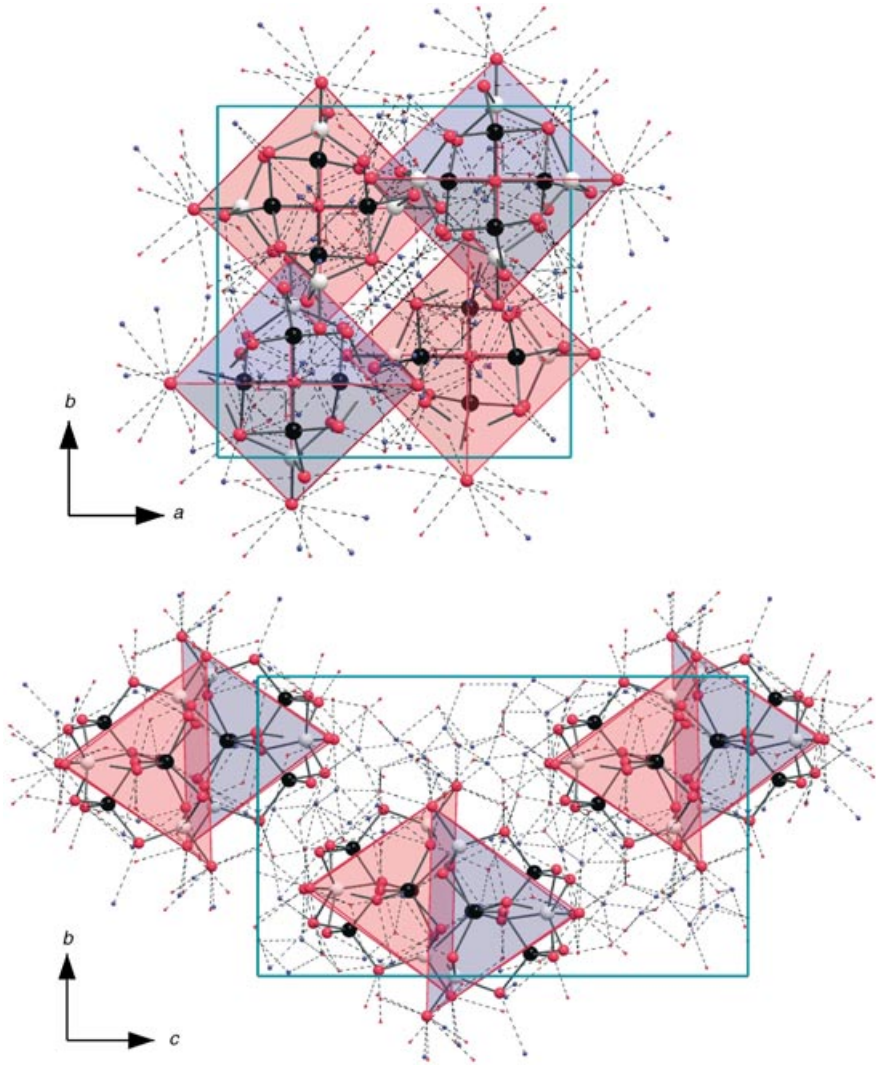

Figure 2. Part of the crystal packing in **4**. Cd: black, Sn: white, Se: red, K: blue, O: red (small), C: white (small). The shaded tetrahedra were formed by linking the four terminal Se ligands per anion, displaying the position of each [Cd(μ-Se)$_3$] unit above the respective tetrahedral face; red and blue tetrahedra represent cluster anions of each of two orientations with respect to the *c* axis. Selected distances and angles are listed and compared to those of isotypic compounds **2**, **3**, and **5** in Table 2.

In contrast to a number of structurally related, ligand-coordinated binary clusters $[M_8(\mu_4\text{-}E)(ER)_{12}L_4]^{2-}$ (M = Zn, Cd; E = S, Se, Te; L = ER, Cl; R = organic group),[21–24] corresponding $[Mn_8(\mu_4\text{-}E)E_{16-x}L_x]$ or $[Hg_8(\mu_4\text{-}E)E_{16-x}L_x]$ clusters have not been reported until now; the only related compound containing Mn atoms is $[Mn_4Cu_4(\mu_4\text{-}S)(S\mathit{i}Pr)_{12}]^{2-}$ in $[NMe_4]_6[Mn_4Cu_4(\mu_4\text{-}S)(S\mathit{i}Pr)_{12}]\cdot 2[MnCl_4]$,[24] which has a different molecular structure based on an Mn_4Cu_4 heterocubane, in which the twelve Mn–Cu edges are all bridged by μ-S*i*Pr$^-$ ligands.

In the crystal, all anions are of the same enantiomer; the cluster molecules are arranged in two types of stacks, parallel or antiparallel to the *c* axis. They are linked by potassium ions that are additionally coordinated by solvent molecules. The absence of stabilizing ligands, such as phenyl groups or phosphane ligands, enables relatively close approach of the ternary anions. The shortest Se···Se intercluster distances are always found between three μ-Se ligands of one ter-

Table 2. Selected bond lengths [pm] and angles [°] of isotypic compounds **4** and **5** in comparison to those in **2** and **3**.[9c]

	2(Zn)[9c]	**3** (Mn)[9c]	**4** (Cd)	**5** (Hg)
Sn–Se_t[a]	251.9(1), 252.4(1)	251.4(2), 252.0(2)	251.1(2), 251.5(2)	250.9(2), 251.6(2)
Sn–(μ-Se)	251.5(1)–252.6(1)	251.8(2)–252.7(2)	252.1(2)–253.0(2)	252.0(2)–253.3(3)
M–(μ-Se)	246.0(2)–250.5(2)	255.4(2)–258.3(2)	263.7(2)–266.2(2)	263.5(2)–267.6(2)
M–(μ_4-Se)	245.7(1), 246.5(1)	252.8(2), 253.4(2)	260.4(2), 261.2(2)	262.2(1), 262.4(1)
M···M	399.0(2)–406.4(2)	408.3(3)–421.1(3)	420.5(2)–433.0(2)	425.0(2)–434.3(2)
M···Sn	386.5(2)–401.7(2)	395.9(3)–408.2(3)	405.0(3)–415.7(3)	403.9(3)–416.2(2)
Se···Se edges	1058.0(1)–1071.2(1)	1071.4(1)–1086.3(1)	1082.0(3)–1095.6(3)	1080.5(2)–1097.1(3)
Se_t-Sn-Se	105.81(4)–107.61(4)	105.37(6)–107.74(6)	104.72(7)–104.97(6)	104.20(6)–106.25(8)
(μ-Se)-Sn-(μ-Se)	109.73(4)–114.36(5)	110.19(5)–114.39(6)	110.87(6)–115.10(7)	111.38(6)–115.52(7)
(μ-Se)-M-(μ-Se)	106.97(5)–109.56(6)	107.75(8)–112.69(9)	107.76(6)–113.98(6)	108.98(5)–112.93(5)
(μ_4-Se)-M-(μ-Se)	108.31(5)–112.08(5)	106.60(7)–110.77(9)	105.71(5)–109.12(6)	105.01(5)–109.16(5)
Sn-(μ-Se)-M	101.44(4)–105.95(4)	102.45(6)–106.24(7)	103.09(6)–106.45(6)	102.40(5)–106.43(5)
M-(μ_4-Se)-M	108.36(4)–111.05(7)	107.71(11)–112.37(12)	107.68(8)–111.97(8)	108.23(2)–111.66(7)
distances within the coordination sphere[b]				
Se···K	322.5(17)–361.8(14)	321.2(2)–354.3(3)	331.6(11)–374.5(9)	326.7(14)–361.4(11)
K···O	225.1(7)–301.2(4)	241.4(2)–303.1(2)	262.1(16)–372.2(19)	268.3(16)-379.9(11)
Se···O	323.3(10)–389.5(9)	311.3(5)–389.1(7)	318.2(16)–384.3(14)	321.5(14)–362.8(13)
nearest intercluster distances				
Se···Se	359.8(8)–361.1(9)	361.0(5)–361.1(8)	357.5(10)–358.9(11)	355.7(11)–356.4(9)

[a] Se_t denotes terminal selenide ligands. [b] Coordination numbers: K as [K···Se_aO_b] ($a=0$–4; $b=2$, 3, 5, 6): five to seven; Se as [$SeSnCo_a\cdots K_bO_c$] ($a=0$, 1; $b=1$, 2; $c=1$–3 ,5 ,7): five to eight.

nary anion and three opposing ones of the adjacent molecule: 359.8(8)–361.1(9) pm (**2**), 361.0(5)–361.1(8) pm (**3**), 357.5(10)–358.9(11) pm (**4**), and 355.7(11)–356.4(9) pm (**5**).

Crystal structure of 6: Comparison of the compositions of the K/Hg/Sn/Se compounds **5** and **6** not only reveals fewer solvent molecules for **6**, but also indicates formal loss of one complete formula unit of the reactant $K_4[SnSe_4]$; this is consistent with the smaller amount of the chalcogenostannate salt in the reaction mixture affording **6** than was used in the synthesis of **5** [Scheme 1, Eqs. (2) and (3)].

Indeed, the monomeric "$[Hg(\mu_4\text{-}Se)(SnSe_4)_3]^{6-}$" unit in **6** can be derived from the $[Hg(\mu_4\text{-}Se)(SnSe_4)_4]^{10-}$ ion in **5** by formal removal of one $[SnSe_4]^{4-}$ unit; ensuing substitution of the Se(1′) ligands of three adjacent cluster fragments for the lost $[SnSe_4]^{4-}$ group leads to recompletion of the coordination sphere of these three Hg(1) atoms. Three-dimensional continuation of this formal condensation process generates a polymeric network. A part of the ternary substructure of **6** is shown in Figure 3, represented by one formula unit of the anion and its connection to adjacent fragments. Selected bond lengths and angles are given in the caption.

All metal atoms in **6** achieve a distorted tetrahedral coordination geometry. In contrast to the μ_3-bridging mode of the $[SnSe_4]^{4-}$ ligands in **1**–**5**, μ_4-$[SnSe_4]^{4-}$ units each bridge three Hg centers of one monomeric unit and additionally bridge to the next $[Hg_4Sn_3Se_{13}]$ fragment. Thus, μ-Se bridges are formed that link the polycylic $[Hg_4Sn_3Se_{10}]$ fragments consisting of three condensed, barrelane-type $[SeHg_3Se_3Sn]$ cages. These bridges enclose the smallest Sn-(μ-Se)-Hg angle (98.82(18)°) in **6**, which is accompanied by a relatively short (nonbonding) Hg(1)···Sn(1′) distance of 391.8(8) pm (about 12 pm less than the shortest Sn···Hg distance in **5**: 403.9(3) pm).

The Sn–Se bond lengths in **6** are similar to the Sn–(μ-Se) distances in **5**; Hg–(μ_4-Se) bonds (260.0(7), 265.1(4) pm) vary around a value of 262 pm in **5**, whereas the Hg–(μ-Se) distances in **6** (260.4(6)–265.4(7) pm) are slightly shorter on average than in **5**. In contrast to the discrete Hg/Sn/Se anions in **5**, which have only pseudo-C_3 rotational symmetry, each cluster fragment, and thus the whole ternary network in **6**, has crystallographic C_3 site symmetry, but with a much stronger distortion in the direction of the crystallographic *c* axis, as can be seen from the structural parameters of the compressed, inner [Hg_4(μ_4-Se)] unit.

The existence of compound **5** and general agreement between the structural parameters of **4** and **5** exclude steric problems as a reason for the existence of the coordination polymer as a structural alternative. It is still unclear whether the formation of **5** represents a condensation process following preliminary detachment of $[SnSe_4]^{4-}$ groups from discrete $[Hg_4(\mu_4\text{-}Se)(SnSe_4)_4]^{10-}$ ions, or whether a different pathway is followed in this case when transition metal ions are substituted for potassium ions in the starting material $K_4[SnSe_4]$.

Uniform orientation of all "$[Hg_4Sn_3Se_{13}]^{6-}$" fragments in the crystal lattice produces a very regular, porous, three-dimensional network embedding the counterions and solvent molecules. Figure 4 illustrates the formal transition from discrete $[Hg_4Sn_4Se_{17}]^{10-}$ ions in **5** to the coordination polymer in **6**.

The three-dimensional linkage of the $[Hg_4Sn_3Se_{13}]$ units leads to the formation of three groups of parallel channels running through the crystal along [1,−1,−1] (see Figure 4),

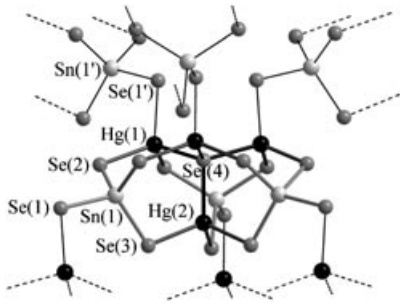

Figure 3. Part of the ternary anionic structure of **6**. Thick bonds highlight the fragment of a discrete anion as in **5**; narrow and dashed bonds denote connections to adjacent fragments and continuation of the structural motif. Selected distances [pm] and angles [°]: Sn(1)–Se(1) 250.3(7), Sn(1)–Se(2,3) 252.5(8)–253.2(6), Hg(1)–Se(1) 265.4(7), Hg(1)–Se(2) 260.4(6), Hg(1)–Se(4) 265.1(4), Hg(2)–Se(3) 265.3(6), Hg(2)–Se(4) 260.0(7), Hg(1)···Hg(2) 416.9(8), Hg(1)···Hg(1) 443.3(7), Hg(1)···Sn(1′) 391.8(8), Hg(1,2)···Sn(1) 407.4(8)–409.7(9); Se(1)-Sn-Se(2,3) 101.11(18)–112.31(14), Se(2,3)-Sn-Se(2,3) 112.91(19)–115.23(17), Se(2,3)-Hg-Se(1,2,3) 107.30(18)–112.56(15), Se(4)-Hg-Se(1,2,3) 100.92(19)–111.56(17), Sn-Se(2,3)-Hg 103.82(20)–105.84(21), Sn-Se(1)-Hg 98.82(18), Hg(1)-Se(4)-Hg(2) 105.11(19), Hg(1)-Se(4)-Hg(1) 113.46(17).

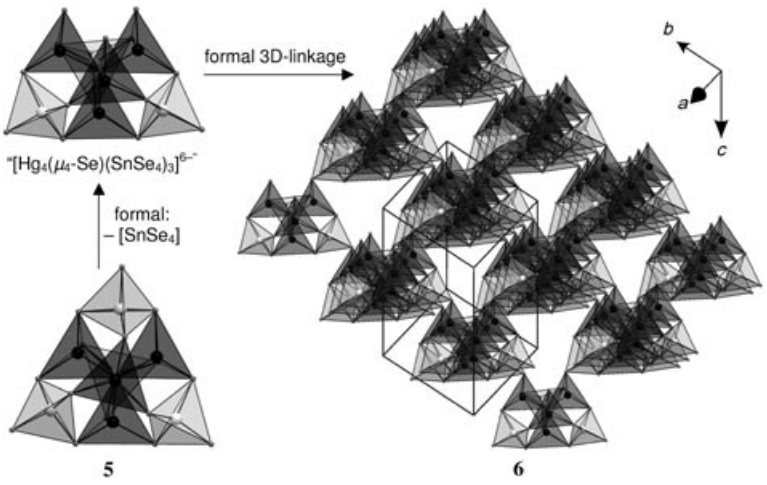

Figure 4. Derivation of a monomeric "$[Hg_4(\mu_4\text{-}Se)(SnSe_4)_3]^{6-}$" unit in **6** by formal removal of an $[SnSe_4]^{4-}$ group from a discrete $[Hg_4(\mu_4\text{-}Se)(SnSe_4)_4]^{10-}$ ion in **5** (top) and formal polymerization to the anionic Hg/Sn/Se network in **6** (bottom; view approximately along [1,−1,−1]); Hg: black, Sn: white, Se: gray. For clarity, three-coordinate Hg atoms in **6** are represented as $[HgSe_3\square]$ tetrahedra.

$[^1/_2,1,-^1/_2]$, and $[1,^1/_2,^1/_2]$. The channel dimensions are approximately 400×700 pm, and the walls are formed by Se atoms, which interact with K^+ counterions in the channels that are additionally coordinated by H_2O molecules. Coordination numbers within the coordination spheres are: K: seven (1 O, 6 Se atoms; K···Se 343.8(7)–401.8(9) pm; K···O 280.4(8), 302.9(8) pm); Se: four (1 Sn, 1 Co, 2 K atoms) or six (1 Sn, 1 Co, 4 K atoms or 1 Sn, 1 Co, 2 K, 2 O atoms; Se···O (H bridges) 319.6(9), 322.7(9) pm); O: four (2 K, 2 H atoms). The MeOH molecules do not coordinate; they are situated at the crossing points of the three sets of channels.

In contrast to the synthesis of the M/E′/E phases[6] quoted at the outset and the related compounds $(CP)_{4-2x}[M_xSnSe_4]$ (CP = cetylpyridinium; x = 1–1.2; M = Mn, Zn, Cd, Hg),[26] $(CP)_{1.4}[Zn_{1.3}Sn_2S_6]$,[27] $(CP)_{1.2}[Cd_{1.4}Sn_2S_6]$,[27] and $A_2[Hg_3E'_2S_8]$ (A = Rb, Cs; E′ = Ge, Sn),[28] the preparation of **6** represents the first reaction of a chalcogenostannate and a transition-metal component that leads to the formation of a infinite network under standard pressure, at room temperature, and without the addition of structure-directing tenside molecules. However, the specific aggregation of the present ions and solvent molecules, which depends on the reaction conditions, mainly the polarity of the solvent, might be viewed as a structure-determining effect too.

Besides the occurrence of the novel type of Hg/Sn/Se network based on ternary cluster fragments, compound **6** is, to our knowledge, the first compound in which a μ_4-type linkage of transition-metal ions through ortho-selenostannate anions has been structurally characterized. Known phases containing μ_4-bridging $[E'S_4]$ (E′ = Ge, Sn) or $[GeE_4]$ groups (E = S, Se), for example, $A_2[Hg_3E'_2S_8]$ (A = Rb, Cs; E′ = Ge, Sn),[28a] that are accessible by solvothermal or flux techniques from the elements or binary chalcogenides form networks by one-, two-, or three-dimensional linkage of $[E'E_4]$ and $[ME_4]$ tetrahedra. However, most of the other compounds that feature porous networks, except the above cited examples, contain larger $[E'_4E_{10}]^{4-}$ ions as spacers between transition metal centers. During revision of the manuscript, an analogous, but solvent-free, Cd/Sn/Se compound was published; it was synthesized by fusion/solvothermal extraction of K_2Se, Cd, Sn, and Se.[28b]

Crystal structure of 7: Compound **7** is the first solvent-free phase to be prepared by the method described here. Whereas solvent molecules remain in the salt of the coordination polymer in **6**, as a reminder of its synthesis in solution, by contrast no H_2O or MeOH molecules are needed for the stabilization of the quaternary phase **7**. The ternary substructure is formed formally by *trans*-edge-sharing $[SnSe_4]^{4-}$ and $[HgSe_4]^{6-}$ tetrahedra that alternate along one-dimensional strands parallel to the crystallographic *c* axis. Such SiS_2-type chains are not rare in the structures of metal chalcogenide or chalcogenido metalate compounds. Strands with one sort of metal atom have been observed in solids such as $ASnSe_3$ (A = Na, K)[29,30] $KFeS_2$,[31] and TlE (= $Tl^{I}(Tl^{III}S_2)$; E = S, Se).[32] Furthermore, the last-named is a structural relative crystallizing in the space group *I*4/*mcm*. Its symmetry is reduced by formal transition to the structure of **7**, which crystallizes in the subgroup $I\bar{4}2m$, as a result of the defined occupation of the metal sites by Hg or Sn. As a third variation of the $[SnSe_4]^{4-}$ coordination modes, the ortho-chalcogenostannate anions in **7** act as bridges between two metal centers with formation of $[HgSe_2Sn]$ four-membered rings. Figure 5 shows views of the crystal packing in **7** along and perpendicular to the $^1_\infty\{[HgSnSe_4]^{2-}\}$ strands; selected structural parameters are given in the caption.

The $^1_\infty\{[HgSnSe_4]^{2-}\}$ chains that follow the $\bar{4}$ axes at the edges of the unit cell and those that follow the $\bar{4}$ axes through the center of the *ab* plane are shifted by *c*/2 with respect to each other; thus, not only Hg and Sn atoms within one strand but also those of adjacent anionic chains have only atoms of the other metal type as nearest neighbors. In contrast to **5** and **6**, the tetrahedral coordination geometry at the metal centers is highly distorted. Coordination of the K^+ ions by eight nearest Se atoms within a range of 340.9(2)–350.5(2) pm produces tetragonal antiprisms as coordination polyhedra that are slightly flattened in the *c* direction.

Compound **7** is structurally related to some compounds containing ortho-tellurostannate groups: $K_2[Ag_2SnTe_4]$,[34a] synthesized by the K_2Te/Te flux technique from K_2Te, Ag, Sn, and Te, and $[Mn(en)_3][CdSnTe_4]$[34b] (en = 1,2-diaminoethane) and $K_2[HgSnTe_4]$,[34c] which were prepared from SnTe, Te, $MnCl_2$, and $CdCl_2$, and from $K_4[SnTe_4]$ and $HgCl_2$ by solvothermal synthesis in en. These phases are also based on one-dimensional chains, two of which differ from those in **7**: the first contains two independent Ag atomic sites,

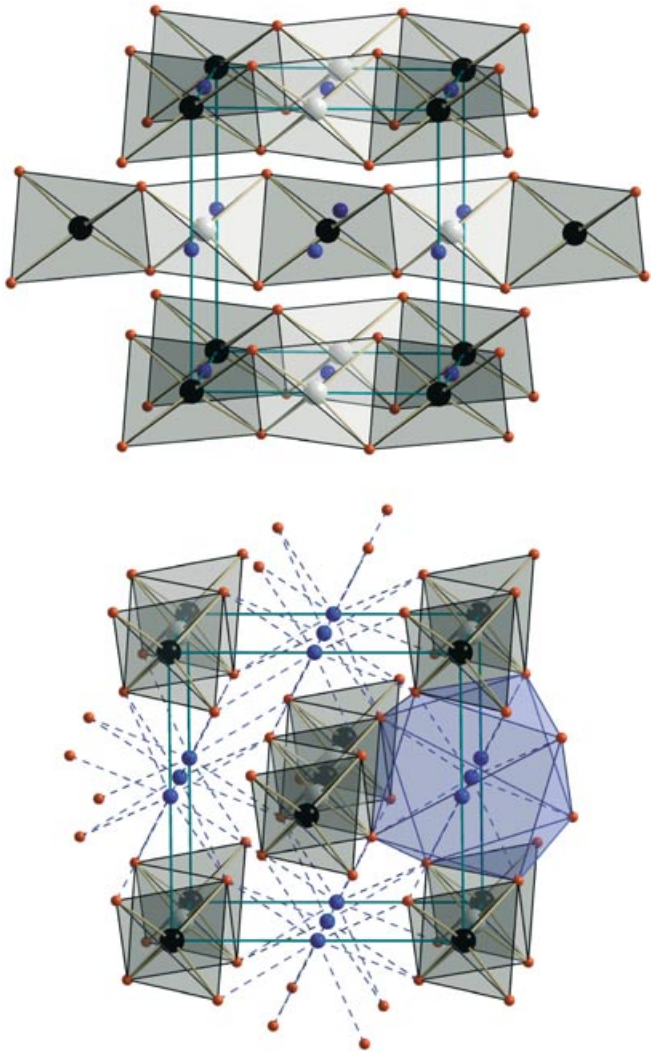

Figure 5. Parts of the crystal packing in **7** along (approximately) [1,0,0] (left) and [0,0,1] (right), emphasizing the tetrahedral $[HgSe_4]$ and $[SnSe_4]$ units; Hg: black, Sn: white, Se: red, K: blue. On the right-hand side, the distorted tetragonal-antiprismatic coordination sphere of the K^+ ions is illustrated by dashed lines and blue polyhedra. Selected distances [pm] and angles [°]: Sn–Se 256.1(4), Hg–Se 268.7(4), Hg···Sn 347.5(3), K···Se 340.9(2)–350.5(2); Se-Sn-Se 100.21(16), 114.29(9), Se-Hg-Se 93.98(15), 117.73(9), Sn-Se-Hg 82.90(9).

only one of which adopts tetrahedral coordination geometry; in the second phase, linkage via *cis* edges of the $[SnTe_4]$ units and *trans* edges of the $[CdTe_4]$ groups lead to the formation of an infinite zig-zag chain. Other related compounds such as $K_2[Ag_2SnSe_6]$[35] and $K_2[MnSn_2Se_6]$[36] have $[Sn_2Se_6]^{4-}$ ions as bridges between Ag or Mn centers in one-dimensional chains. However, to our knowledge, no compounds that feature bridging ortho-selenostannate anions $[SnSe_4]^{4-}$ between two transition metal ions, as observed in **7**, have been described to date.

Electronic structures and static magnetic properties of 2–5: In spite of the relatively small molecular sizes of the ternary $[M_4(\mu_4\text{-Se})(SnSe_4)_4]^{10-}$ ions in **2–5**, and the presence of ($[SnSe_4]^{4-}$-linked) $3d^5$, $3d^{10}$, $4d^{10}$, or $5d^{10}$ transition-metal ions that are usually inconspicuous with respect to their optical absorption, these compounds form intensely colored solutions and crystals. To gain insight into the electronic structures of the four isotypic systems, we recorded UV-visible spectra of these compounds and performed DFT[14] calculations on the anions. Additionally, the static magnetic behavior of the $3d^5$ system **3** was investigated by magnetic susceptibility measurements and ESR spectrometry.

UV-visible spectra of 2–5: Solid-state UV-visible spectra of **2–5** are shown in Figure 6. Corresponding data that have been extracted from the graphs and data of related compounds are listed in Table 3.

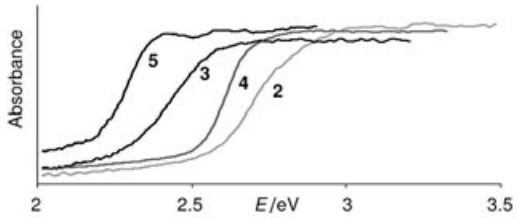

Figure 6. UV-visible spectra of **2**,[9c] **3**,[9c] **4**, and **5** in the solid state, recorded as suspensions of single-crystalline material in Nujol.

Table 3. Optical absorption energies E extracted from the UV-visible spectra of **2–5** and optical gaps of related binary solids.[37]

	2 (Zn)	**3** (Mn)	**4** (Cd)	**5** (Hg)
E_{max} [eV]	2.90	2.56	2.68	2.36
crystal color	light yellow	orange	yellow	orange
E_{onset} [eV]	2.57	2.27	2.53	2.21
optical gap of MSe[37] [eV]	2.7	2.5	1.7	-0.06[a]

[a] HgSe is a so-called inverse band gap semiconductor.[37]

Plateaus of maximum absorbance are observed at E_{max} = 2.36–2.90 eV, which corresponds to the visible color of the compounds. Before reaching the plateaus, the absorbance increases over a range of 0.15–0.28 eV (30–60 nm) from the onset of absorption E_{onset}. We assign this onset to the lowest possible electronic excitation in the respective system, that is, the energy difference between highest occupied and lowest unoccupied molecular orbitals of the optically active components. According to the spectra, these gaps are in the range 2.21–2.57 eV.

Whereas for the Cd and Hg containing phases **4** and **5** the values are still well separated from the optical gaps of the binary MSe solids, the Zn and Mn species **2** and **3** show gaps that are very close to those in the metal selenides,[37] although only very small (distorted) parts of the Wurzite-type topology of the MSe phases are represented by the inner $[(\mu_4\text{-Se})M_4(\mu\text{-Se})_{12}]$ cores of the ternary anions. This is a result of the partial substitution of Sn (optical gap of $SnSe_2$: 1.2 eV[37]) for the d^{10} transition metal atoms in the $[M_8E_{17}]$ clusters, which causes a significant change of the electronic situation. Gaps that are relatively small for the molecular size are therefore observed.

The structurally related binary Zn/Se and Cd/Se clusters cited above are colorless and accordingly show significantly larger electronic excitation energies than **2** or **4**;[22,24] for $[Cd_8(\mu_4\text{-Se})(SePh)_{14}(PnPr_2Ph)_2]$; the gap was spectroscopi-

cally determined to be 3.8 eV.[38] This difference must be attributed in part to the absence of a ligand shell in **2**–**5**: ligand-free CdSe nanoparticles of a similar diameter (12 Å vs 11 Å in **4**) have a gap of about 3.0 eV.[39] The remaining decrease in the excitation energy should be finally assigned to the mixed-metal nature of **2**–**5**.

Additionally, the values are on the same order of magnitude as the gaps that were observed for the related mesostructured compounds $(CP)_{4-2x}[Mn_xSnSe_4]$.[26] This indicates that both separation of discrete M/Sn/Se anions by (solvated) K^+ ions and incorporation of tenside micelles in a three-dimensional aggregation affect the optical behavior in a similar manner. As expected, the energy differences are somewhat smaller than those observed for the sulfur analogues $K_4[Zn_4Sn_4S_{17}]$ (3.1 eV) and $K_4[Mn_4Sn_4S_{17}]$ (2.3 eV).[11]

The UV-visible spectra of **2**–**5** show that the spectrum of the d^5 compound **3** is rather exceptional: the gap for this compound does not fit into a trend which parallels ionic or covalent radii or atomic numbers.

Quantum chemical investigations: To examine the electronic situation that we claim to be responsible for the different absorption behavior of **3** compared to **2**, **4**, and **5** and to obtain insight into the spin state, that is, the magnetic properties of **3**, quantum chemical investigations were carried out. The electronic structures of the four isostructural $[M_4(\mu_4\text{-Se})(SnSe_4)_4]^{10-}$ ions (M = Zn, Mn, Cd, Hg) were studied and compared by DFT[14] calculations, which proved to be suitable for ternary M/Sn/Se anions.[9] The calculations were performed with the program package TURBOMOLE,[40] using the COSMO model[41] to compensate for the highly negative charge on the anions by simulation of mirror charges (see Experimental Section). Simultaneous optimization of electronic and geometric structures resulted in reasonable structural parameters (maximum deviations of the M–Se bonds: 1.3–5.3 pm in **2**, 0.6–2.0 pm in **3**, 3.2–6.5 pm in **4**, 7.2–12.7 pm in **5**; maximum deviations of the Sn–Se bonds: 3.7–7.3 pm in **2**, 3.9–8.0 pm in **3**, 4.0–7.6 pm in **4**, 4.1–7.8 pm in **5**). The anions of the d^{10} transition metal compounds **2**, **4**, and **5** were shown to be closed-shell systems, as expected; the anion of **3** had to be treated as an open-shell system by using the unrestricted Kohn–Sham (UKS) model.

A significant difference between the d^{10} systems and the d^5 system is evident from Mulliken analyses of the frontier orbitals, which are of interest for the optical spectra: whereas in the d^{10} closed-shell anions with M = Zn, Cd, or Hg the metal orbitals do not contribute to the highest molecular orbitals,[42] significant contribution of Mn d orbitals (ca. 30%) is evident in each of the highest occupied orbitals in the d^5 cluster anion of **3**. This is probably a consequence of lower energies for the atomic orbitals of Zn^{2+}, Cd^{2+}, or Hg^{2+} relative to Mn^{2+} with respect to their direct bonding partner Se^{2-} in $[SnSe_4]^{4-}$. Thus, the UV-visible absorption and colors of **2**, **4**, and **5** should be explained by pure charge-transfer transitions from filled Se p orbitals to empty M- or Sn-based orbitals, whereas in **3**, a significant influence of the occupied metal atomic orbitals must be considered. The different molecular orbital scheme gives rise to a different behavior in the absorption process in **3** and thus to an excitation energy that does not follow the trend for the anions with the d^{10} metal atoms, as observed experimentally.

The UKS calculation revealed 20 unpaired electrons. Analysis of the spin density (i.e., difference of densities for alpha and beta spins) shows that these are clearly localized at the four Mn centers, in accord with the d^5 configuration. However, the four d^5 shells do not have the same spin orientation in the calculated ground state: the unpaired electrons of two Mn atoms have one spin orientation, whereas those at the other two Mn atoms have the opposite spin. This corresponds to an $S = 0$ state, with antiferromagnetic coupling of the Mn^{II} centers, as the energetically most favorable. Figure 7 shows the spin density calculated for the local minimum. Surplus of alpha and beta spins is represented by red and blue clouds, respectively.

Thorough analysis of other possible spin states of the anion in **3** revealed that excited states with $S = 5$ and $S = 10$, which also fulfill the aufbau principle, are 0.2 or 0.3 eV less favorable.

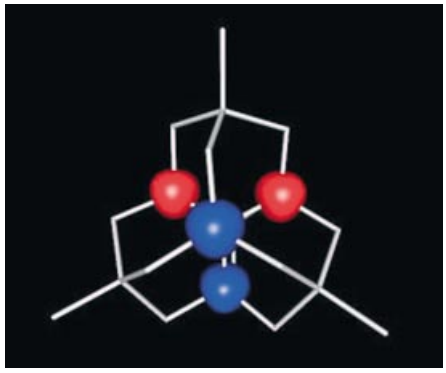

Figure 7. Plot of the spin density of the calculated anion $[Mn_4(\mu_4\text{-Se})(SnSe_4)_4]^{10-}$. Spin densities (i.e., difference of densities for alpha (red) and beta (blue) spins) are drawn to 0.4 $e^- Å^{-3}$.

Magnetism of 3: Susceptibility measurements were performed on a polycrystalline sample of **3** (18.10 mg) between $T = 1.8$ and 300 K at 1000 Oe. Figure 8 depicts the χ versus T plot. The magnetic susceptibility increases from 300 K to reach a maximum at 17 K (0.054 emu mol^{-1}) before decreasing to 0.03 emu mol^{-1} at 3.5 K. A further decrease in temperature leads to an increase in the magnetic susceptibility typical for Curie-like paramagnetic impurities.

This global paramagnetic behavior was analyzed by considering the $[Mn_4(\mu_4\text{-Se})(SnSe_4)_4]^{10-}$ units to be well isolated in the crystal packing, with a closest Mn···Mn distance between the clusters of about 5.1 Å. Therefore, intercluster magnetic exchanges were not considered. Based on the molecular description of the $[Mn_4(\mu_4\text{-Se})(SnSe_4)_4]^{10-}$ unit, the possible exchange pathways J are shown in Scheme 2, in which only direct Se bridges are taken into account.

Given the similarity of the selenium bridges between Mn^{II} magnetic centers (Table 4), we simplified the model by considering all the magnetic exchange interactions J between the metal ions to be equal.

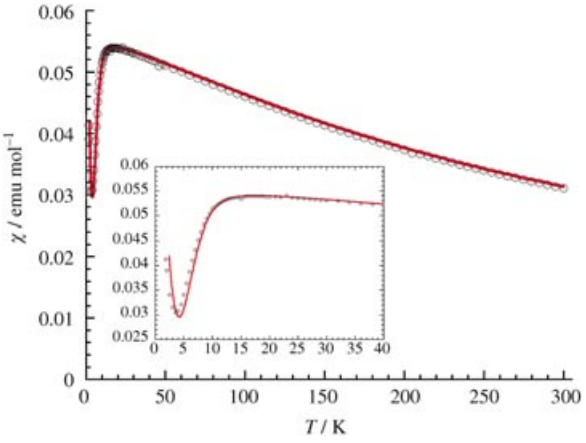

Figure 8. χ versus T plot for a polycrystalline sample of **3**. Inset: zoom of the χ versus T plot in the low-temperature region below 40 K.

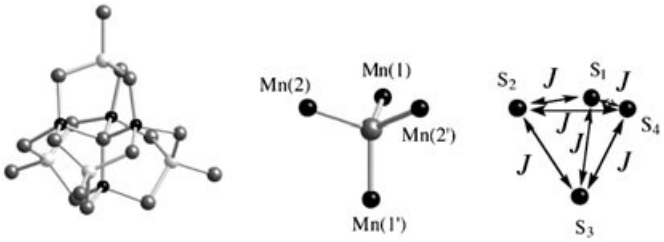

Scheme 2. Exchange pathways of magnetic coupling in **3**.

Table 4. Distances [pm] and angles [°] of relevance for the magnetic coupling in **3**.

Magnetic coupling	Mn-(μ_4-Se)-Mn	Mn–(μ_4-Se)
Mn(1)–Mn(1′)	107.71(11)	252.8(2)
Mn(2)–Mn(2′)	112.37(12)	253.4(2)
Mn(1)–Mn(2) or Mn(1′)–Mn(2′)	110.01(7)	252.8(2), 253.4(2)
Mn(1)–Mn(2′) or Mn(1′)–Mn(2)	108.32(6)	252.8(2), 253.4(2)

Therefore, the magnetic data were analyzed with the Hamiltonian of Equation (5) in which $j>i$ and S_i is the spin of an individual Mn^{II} metal ion (note that in the tetrahedral coordination sphere, the d^5 Mn^{II} is known to be in its high-spin state: $S=5/2$).

$$H = -2J \sum_{i=1,\, j=2}^{4} S_i S_j \qquad (5)$$

The complicated topology of the magnetic pathways precludes a simple calculation of the spin levels of the cluster by Kambe's method;[43] hence, we used a more general procedure developed by Clemente-Juan et al. (MAGPACK program).[44] In addition to the susceptibility calculated from the above Hamiltonian $\chi_{tetramer}$, we had to consider a Curie contribution from isolated $S=5/2$ Mn^{II} ions as impurities to be able to reproduce the low temperature behavior [Eq. (6)].

$$\chi = (1-\rho)\chi_{tetramer} + \rho\frac{35\,Ng^2\mu_B^2}{12\,k_B T} \qquad (6)$$

The best set of parameters that fitted the experimental magnetic data was $g=2.0$, $J/k_B=-12.1(2)$ K, and $\rho=0.023$ (solid line in Figure 8). The value of the g factor was confirmed by ESR measurements on a polycrystalline sample. At room temperature, a single Lorentzian resonance line was observed at $g=2.015$ with a line width ΔH of 640 Oe. On decreasing the temperature, the g factor remains constant and ΔH increases to 2400 Oe at 4.2 K. The estimation of the susceptibility from double integration of the resonance line confirmed the magnetometer measurements shown in Figure 8. Fitting of the magnetic susceptibility revealed a significant antiferromagnetic interaction ($J/k_B=-12.1(2)$ K) between the Mn^{II} ions through the Se bridge. The results show that the ground state of the $[Mn_4(\mu_4\text{-}Se)(SnSe_4)_4]^{10-}$ cluster is a singlet with a first excited state ($S=1$) at 24.2 K. Compound **3** is to our knowledge the first compound with an $[Mn_4Se]$ fragment to be investigated by magnetic measurements, but antiferromagnetic coupling between tetrahedrally coordinated Mn centers was also observed in $K_2[MnSnS_4]$,[6c] albeit based on a two-dimensional Mn/Sn/S network with μ-bridging sulfur ligands instead of μ_4-bridging ligands .

Conclusion

We have shown that it is possible to use the synthetic method that was first described for the syntheses of quaternary Co, Zn, and Mn compounds **1**–**3** for reactions with salts of the heavier transition metals cadmium and mercury by suitable variation of the reaction conditions. In this way, novel quaternary compounds were synthesized that contain purely inorganic, ternary anionic M/Sn/Se substructures with M = Cd or Hg.

By preparing compounds **4** and **5**, which incorporate discrete $[M_4(\mu_4\text{-}Se)(SnSe_4)_4]^{10-}$ ions (**4**: M = Cd, **5**: M = Hg), we completed a homologous series of isotypic compounds **2** (M = Zn), **4**, and **5**. The phases show unexpected colors and optical gaps given the relatively small molecular size (25 atoms) of the anions containing d^{10} metal centers. Quantum chemical investigations at the DFT level suggest the absorption behavior of the anions with d^{10} metal atoms to have mainly Se(p)→M(d) charge-transfer character. In contrast, the electronic structure of isotypic d^5 metal compound **3**, containing analogous Mn/Sn/Se anions, differs in being an open-shell system that displays significant metal d-orbital contribution to the highest molecular orbitals. Accordingly, the optical absorption does not follow the trend of the Zn, Cd, and Hg compounds. For the anion in **3**, 20 unpaired electrons were calculated that represent the four d^5 shells of the Mn atoms. The quantum chemical studies and experimental investigations of the magnetic susceptibility of a polycrystalline sample of **3** agree in that an $S=0$ ground state resulting from significant antiferromagnetic interactions ($J/k_B=-12.1(2)$ K) between the Mn^{II} metal ions through the ligand bridge, was determined in both cases.

In contrast to the experiments with Zn, Mn, or Cd salts, reactions with $Hg(OAc)_2$ show a variation in the product distribution when the reaction conditions are slightly

changed. It was thus possible to isolate and structurally characterize two further quaternary compounds containing Hg/Sn/Se substructures. In **6**, this is a three-dimensional network of formally condensed fragments of the discrete cluster anions observed in **5**, namely, "$[Hg_4(\mu_4\text{-}Se)(SnSe_3)]^{6-}$". The anionic substructure in **7** does not show a relation to the d^{10} metal/Sn/Se anions isolated so far, but forms one-dimensional strands of alternating, edge-sharing $[HgSe_4]$ or $[SnSe_4]$ tetrahedra.

In future investigations we intend to investigate possible nonlinear optical properties of the chiral compounds **2**–**5**. We also plan to gain insight in solution processes that are so far unknown, by means of dynamic light scattering and ESI mass spectrometry. Furthermore, we aim to explore whether new variations of reactant combinations and/or reaction conditions allow the isolation of further quaternary phases with ternary substructures and to study how these parameters influence the actually observed structural motifs and their physical properties.

Experimental Section

General: All synthesis steps were performed with strict exclusion of air and moisture (N_2 atmosphere on a high-vacuum, double-manifold Schlenk line or Ar atmosphere in a glove box). Methanol, THF, and toluene were dried and freshly distilled prior to use; water was degassed by applying dynamic vacuum (10^{-3} Torr) for several hours. $K_4[SeSe_4]\cdot 1.5$ MeOH was synthesized as previously described;[9c] $CdCl_2$ and $Hg(OAc)_2$ were purchased from Merck (>98%).

Synthesis of $[K_{10}(H_2O)_{16}(MeOH)_{0.5}][Cd_4(\mu_4\text{-}Se)(SnSe_4)_4]$ (4): $K_4[SnSe_4]\cdot 1.5$ MeOH (0.192 g, 0.300 mmol) was suspended in MeOH (5 mL) and added to a solution of $CdCl_2$ (0.043 g, 0.240 mmol) in H_2O (5 mL), whereupon the reaction mixture immediately turned light yellow, and a similarly colored powder precipitated. After stirring for 24 h, the solution was removed from the precipitate by decanting, the yellow solid was redissolved in water (10 mL) and layered with THF (10 mL). Over one week, yellow crystals of **4** formed selectively, while layering of the decanted reaction solution only yielded crystals of the co-product $[K_4(MeOH)_4][Sn_2Se_6]$.[9] Yield of **4**: 0.133 g (0.045 mmol, 78% based on $[SnSe_4]^{4-}$); elemental analysis calcd (%): C 0.20, H: 1.18; found: C 0.20, H 1.19.

Synthesis of $[K_{10}(H_2O)_{16}(MeOH)_{0.5}][Hg_4(\mu_4\text{-}Se)(SnSe_4)_4]$ (5): $K_4[SnSe_4]\cdot 1.5$ MeOH (0.112 g, 0.175 mmol) was suspended in MeOH (5 mL) and added to a solution of $Hg(OAc)_2$ (0.045 g, 0.140 mmol) in H_2O (5 mL), whereupon a black precipitate formed immediately. After stirring for 24 h, the precipitate was removed and the filtrate layered with THF (10 mL). Small, orange truncated octahedra of **5** formed, besides small amounts of $[K_4(MeOH)_4][Sn_2Se_6]$[9] after one week. Yield of **5**: 0.064 g (0.019 mmol, 66% based on $[SnSe_4]^{4-}$); elemental analysis calcd (%): C 0.18, H 1.04; found: C 0.18, H 1.02.

Synthesis of $[K_6(H_2O)_3][Hg_4(\mu_4\text{-}Se)(SnSe_4)_3]\cdot$MeOH (6): $K_4[SnSe_4]\cdot 1.5$ MeOH (0.096 g, 0.150 mmol) was suspended in MeOH (5 mL) and added to a solution of $Hg(OAc)_2$ (0.048 g, 0.150 mmol) in H_2O (5 mL), with immediate formation of a black, insoluble precipitate. After stirring for 24 h, the precipitate was removed and the filtrate layered with THF (10 mL). Over two weeks, small orange cuboids of **6** crystallized together with small quantities of $[K_4(MeOH)_4][Sn_2Se_6]$.[9] Yield of **6**: 0.029 g (0.011 mmol, 38% based on $[SnSe_4]^{4-}$); elemental analysis calcd (%): C 0.48, H 0.40; found: C 0.49, H 0.40.

Synthesis of $K_2[HgSnSe_4]$ (7): $K_4[SnSe_4]\cdot 1.5$ MeOH (0.096 g, 0.15 mmol) was suspended in methanol (5 mL) and added to a solution of $Hg(OAc)_2$ (0.048 g, 0.150 mmol) in a mixture of MeOH (4.5 mL) and H_2O (0.5 mL). A black, insoluble precipitate formed immediately. After stirring overnight, the precipitate was removed by filtration, and toluene (10 mL) was allowed to flow under the filtrate. After one week, large amounts of $[K_4(MeOH)_4][Sn_2Se_6]$[9] had formed; after nine weeks, crystallization of small ruby-red rhombuses of **7** started. Yield of **7**: 0.014 g (0.02 mmol, 26% based on $[SnSe_4]^{4-}$).

Quantum chemical investigations: DFT calculations[14] were performed using the program package TURBOMOLE[40] (RIDFT program,[45] Becke–Perdew functional (BP86)[46]). Basis sets were of TZVP quality (triple-zeta valence plus multiple polarization functions).[45b] Relativistically corrected effective core potentials (ECP) were used for the Sn, Cd, and Hg atoms.[47] Compensation of the negative charges of all calculated molecules was achieved by simulating mirror charges using the COSMO model.[41] Suitability of these methods with satisfactory accuracy regarding experimental structures was previously shown in investigations on the anion of **1**.[9a] The use of the unrestricted Kohn–Sham (UKS) modus allowed for systematic investigations of ground-state occupations. The reliability of the UHF result was confirmed by an $\langle S\cdot S\rangle$ value of 110.059 corresponding to 20 excess alpha spins. All geometry optimizations were performed without symmetry restrictions (C_1 symmetry); therefore, convergence into local minimum structures can be assumed. However, the optimizations ended up at nearly T_d symmetric molecules; this indicates the key role of crystal packing for the chirality of the experimentally observed anions. Visualization of the spin density was achieved by means of the gOpenMol program.

ESR investigations and magnetic measurements: ESR spectra were recorded on an X band (9.3 GHz) Bruker ESP300E spectrometer equipped with an ESR900 cryostat (3.8–300 K) from Oxford Instruments. The magnetic susceptibility measurements were obtained using a Quantum Design SQUID magnetometer MPMS-XL. The sample was prepared in a glove box under argon and packed in a sealed plastic bag. The magnetic data were corrected for the sample holder and the diamagnetic contribution calculated from the Pascal constants ($-9.4\cdot 10^{-4}$ emu mol^{-1}).[48]

Acknowledgement

This work was supported by the state of Baden-Württemberg (Margarete-von-Wrangell habilitation fellowship for S.D.), the Deutsche Forschungsgemeinschaft, and the Fonds der Chemischen Industrie. The authors furthermore acknowledge financial support by the Université de Bordeaux I, the CNRS, and the Conseil Regional d'Aquitaine. We are indebted to Dr. C. E. Anson for valuable discussion and help with the manuscript. The authors are also grateful to J. M. Clemente-Juan for teaching and providing the MAGPACK package and to X. Le Goff for performing the ESR measurements. Finally, generous support of our research activities by Prof. Dr. D. Fenske and provision of computational equipment by Prof. Dr. R. Ahlrichs is very much acknowledged.

[1] Reviews: a) J. Wachter, *Angew. Chem.* **1998**, *110*, 782–800; *Angew. Chem. Int. Ed.* **1998**, *37*, 750–768; b) M. G. Kanatzidis, A. C. Sutorik, *Prog. Inorg. Chem.* **1995**, *43*, 151–265; c) G. W. Drake, J. W. Kolis, *Coord. Chem. Rev.* **1994**, *137*, 131–178.

[2] a) F. Jellinek in *Inorganic Sulfur Chemistry* (Ed.: G. Nickless), Elsevier, Amsterdam **1968**, pp. 669–747; b) F. Hulliger, *Struct. Bonding* **1968**, *4*, 83–229.

[3] B. Schiemenz, F. Ettel, G. Huttner, L. Zsolnai, *J. Organomet. Chem.* **1993**, *458*. 159–166.

[4] R. Hauser, K. Merzweiler, *Z. Anorg. Allg. Chem.* **2002**, *628*, 905–906.

[5] A. Loose, W. S. Sheldrick, *Z. Naturforsch. Teil B* **1997**, *52*, 687–692.

[6] a) P. N. Trikalitis, T. Bakas, V. Papaefthymiou, M. G. Kanatzidis, *Angew. Chem.* **2000**, *112*, 4732–4736; *Angew. Chem. Int. Ed.* **2000**, *39*, 4558–4562; b) P. N. Trikalitis, K. K. Rangan, M. G. Kanatzidis, *J. Am. Chem. Soc.* **2002**, *124*, 2604–2613; c) G. D. Albertelli II, J. A. Cowen, C. N. Hoff, T. A. Kaplan, S. D. Mahanti, J. H. Liao, M. G. Kanatzidis, *Phys. Rev. B* **1997**, *55*, 11056–11059; d) M. J. McLachlan, N. Coombs, G. A. Ozin, *Nature* **1999**, *397*, 681–684.

[7] M. Tampier, D. Johrendt, *Z. Naturforsch. Teil B* **1998**, *53*, 1483–1488.

[8] a) S. Dehnen, C. Zimmermann, *Chem. Eur. J.* **2000**, *6*, 2256–2261; b) S. Dehnen, C. Zimmermann, *Eur. J. Inorg. Chem.* **2000**, 1471–

1473; c) C. Zimmermann, S. Dehnen, *Z. Anorg. Allg. Chem.* **2001**, *627*, 847–850; d) C. Zimmermann, C. E. Anson, A. L. Eckermann, M. Wunder, G. Fischer, I. Keilhauer, E. Herrling, B. Pilawa, O. Hampe, F. Weigend, S. Dehnen, *Inorg. Chem.* **2004**, *43*, 4594–4603.

[9] a) C. Zimmermann, M. Melullis, S. Dehnen, *Angew. Chem.* **2002**, *114*, 4444–4447; *Angew. Chem. Int. Ed.* **2002**, *41*, 4269–4272; M. Melullis, C. Zimmermann, C. E. Anson, S. Dehnen, *Z. Anorg. Allg. Chem.* **2003**, *629*, 2325–2329; c) S. Dehnen, M. K. Brandmayer, *J. Am. Chem. Soc.* **2003**, *125*, 6618–6619.

[10] K. O. Klepp, *Z. Naturforsch. Teil B* **1992**, *47*, 411–417.

[11] O. Palchik, R. G. Iyer, J. H. Liao, M. G. Kanatzidis, *Inorg. Chem.* **2003**, *42*, 5052–5054.

[12] H. G. von Schnering, G. Sawitzki, K. Peters, K.-F. Tebbe, *Z. Anorg. Allg. Chem.* **1974**, *404*, 38–50.

[13] L. Erikson, S. Frostang, J. Grins, *Acta Crystallogr. Sect. B* **1990**, *46*, 736–739.

[14] a) R. G. Parr, W. Yang, *Density Functional Theory of Atoms and Molecules*, Oxford University Press, New York **1988**; b) T. Ziegler, *Chem. Rev.* **1991**, *91*, 651–667.

[15] B. Krebs, *Angew. Chem.* **1983**, *95*, 113–134; *Angew. Chem. Int. Ed. Engl.* **1983**, *22*, 113–134.

[16] H. D. Flack, *Acta Crystallogr. Sect. A* **1983**, *39*, 876–881.

[17] Details of the refinement of **4**–**7**. Compounds **4** and **5**: refinement of Cd, Hg, Sn, Se, and nondisordered K atoms by employing anisotropic displacement parameters; one K atom fourfold disordered, one K atomic position half occupied, one O atom twofold (**4**) or threefold (**5**) disordered, assignment of respective split positions, refinement of O, C, and disordered K atomic positions by employing isotropic displacement parameters, H atoms not calculated; compound **6**: refined as racemic twin; even very small crystals seem to be systematically twinned; an additional existence of a drilling of a monoclinic structure (space group *Cm*), which can in principle simulate the rhombohedral symmetry (R. Herbst-Irmer, G. M. Sheldrick, *Acta Crystallogr. Sect. B* **1998**, *54*, 443–449), was checked but did not lead to better results; refinement of Hg, Sn, and Se atomic positions by employing anisotropic displacement parameters, O atoms of coordinating H_2O molecules twofold disordered, both K atoms and C and O atoms of the free MeOH molecule threefold disordered, assignment of respective split positions, refinement of O, C, and K atomic positions by employing isotropic displacement parameters, H atoms not calculated; compound **7**: refined as racemic twin; refinement of Hg, Sn, Se, and K atomic positions by employing anisotropic displacement parameters. CCDC 203729–203731 (**4**–**6**) contain the supplementary crystallographic data for this paper. These data can be obtained free of charge via www.ccdc.cam.ac.uk/conts/retrieving.html (or from the Cambridge Crystallographic Data Centre, 12 Union Road, Cambridge CB2 1EZ, UK; fax: (+44) 1223-336-033; or deposit@ccdc.cam.uk). Further details of the crystal structure investigation for compound **7** can be obtained from the Fachinformationszentrum Karlsruhe, 76344 Eggenstein-Leopoldshafen, Germany, (fax: (+49) 7247-808-666; e-mail: crysdata@fiz-karlsruhe.de) on quoting the depository number CSD-413308.

[18] G. W. Sheldrick, SHELXTL 5.1, Bruker AXS Inc., Madison, WI, USA, **1997**.

[19] R. D. Shannon, *Acta Crystallogr. Sect. A* **1976**, *32*, 751–767.

[20] A. F. Wells, *Structural Inorganic Chemistry*, 4th ed., Clarendon Press, Oxford, **1984**, p. 1013.

[21] a) I. G. Dance, *J. Chem. Soc. Chem. Commun.* **1980**, 818–820; b) I. G. Dance, *Aust. J. Chem.* **1985**, *38*, 1391–1411; c) S. Guo, E. Ding, H. Chen, Y. Yin, X. Li, *Polyhedron* **1999**, *18*, 735–740; d) R. Burth, M. Gelinsky, H. Vahrenkamp, *Inorg. Chem.* **1998**, *37*, 2833–2836.

[22] A. Eichhöfer, D. Fenske, H. Pfistner, M. Wunder, *Z. Anorg. Allg. Chem.* **1998**, *624*, 1909–1914.

[23] a) G. S. Lee, K. J. Fisher, D. C. Craig, M. L. Scudder, I. G. Dance, *J. Am. Chem. Soc.* **1990**, *112*, 6435–6437; b) I. G. Dance, R. G. Garbutt, D. C. Craig, *Inorg. Chem.* **1987**, *26*, 3732–3740; c) K.-L. Tang, X.-L. Jin, S.-J. Jia, Y.-Q. Tang, *J. Struct. Chem.* **1995**, *14*, 399–404.

[24] S. Behrens, D. Fenske, *Ber. Bunsen-Ges.* **1997**, *101*, 1588–1592.

[25] H.-O. Stephan, M. G. Kanatzidis, G. Henkel, *Angew. Chem.* **1996**, *108*, 2257–2259; *Angew. Chem. Int. Ed. Engl.* **1996**, *35*, 2135–2137.

[26] P. N. Trikalitis, K. K. Rangan, T. Bakas, M. G. Kanatzidis, *Nature* **2001**, *410*, 671–675. Structural comparison of **5**–**7** with $(CP)_{1.6}[Hg_{1.2}SnSe_4]$, which also contains $[SnSe_4]^{4-}$-bridged Hg atoms, is not possible due to the lack of a structural determination of this powder phase until now.

[27] K. K. Rangan, P. N. Trikalitis, C. Canlas, T. Bakas, D. P. Weliky, M. G. Kanatzidis, *Nano Lett.* **2002**, *2*, 513–517.

[28] a) G. A. Marking, J. A. Hanko, M. G. Kanatzidis, *Chem. Mater.* **1998**, *10*, 1191–1199; b) N. Ding, D.-Y. Chung, M. G. Kanatzidis, *Chem. Commun.* **2004**, 1170–1171.

[29] a) B. Eisenmann, J. Hansa, *Z. Kristallogr.* **1993**, *203*, 291–292; b) B. Eisenmann, J. Hansa, *Z. Kristallogr.* **1993**, *203*, 293–294.

[30] K. O. Klepp, *J. Solid State Chem.* **1995**, *117*, 356–362.

[31] J. W. Boon, C. H. MacGillary, *Recl. Trav. Chim. Pays-Bas*, **1942**, *61*, 910–920.

[32] J. A. A. Ketelaar, W. H. t'Hart, M. Moerel, D. Polder, *Z. Kristallogr.* **1939**, *101*, 367–368.

[33] W. P. Binnie, M. J. Redman, W. J. Mallio, *Inorg. Chem.* **1970**, *9*, 1449–1452.

[34] a) J. Li, H.-Y. Guo, D. M. Proserpio, A. Sironi, *J. Solid State Chem.* **1995**, *117*, 247–255; b) Z. Chen, R.-J. Wang, J. Li, *Chem. Mater.* **2000**, *12*, 762–766; c) S. S. Dinghara, R. C. Haushalter, *Chem. Mater.* **1994**, *6*, 2376–2381.

[35] H. Guo, Z. Li, L. Yang, P. Wang, X. Huang, J. Li *Acta Crystallogr. Sect. C* **2000**, *57*, 1237–1238.

[36] X. Chen, X. Huang, A. Fu, J. Li, L.-D. Zhang, H.-Y. Guo, *Chem. Mater.* **2000**, *12*, 2385–2391.

[37] O. Madelung, M. Schulz, H. Weiss in *Landoldt-Börnstein, Zahlenwerte und Funktionen in Naturwissenschaften und Technik*, *Vol. 17* (Eds.: K.-H. Hellwege, O. Madelung), Springer, Berlin **1984**; p. 202, p. 236, p. 126, p. 303; p. 208.

[38] V. Soloviev, A Eichhöfer, D. Fenske, U. Banin, *J. Am. Chem. Soc.* **2000**, *122*, 2673–2674.

[39] C. B. Murray, D. J. Norris, .M. G. Bawendi, *J. Am. Chem. Soc.* **1993**, *115*, 8706–8715.

[40] a) R. Ahlrichs, M. Bär, M. Häser, H. Horn, C. Kölmel, *Chem. Phys. Lett.* **1989**, *162*, 165–169; b) O. Treutler, R. Ahlrichs, *J. Chem. Phys.*, **1995**, *102*, 346–354; c) M. von Arnim, R. Ahlrichs, *J. Chem. Phys.* **1999**, *111*, 9183–9190.

[41] a) A. Klamt, *J. Chem. Phys.* **1995**, *103*, 9312–9320; b) A. Schäfer, A. Klamt, D. Sattel, J. C. W. Lohrenz, F. Eckert, *Phys. Chem. Chem. Phys.* **2000**, *2*, 2187–2193.

[42] Highest MOs with metal orbital contribution are about 5.6 eV (M = Zn), 5.4 eV (M = Cd), or 2.2 eV (M = Hg) lower in energy than the respective HOMOs according to Mulliken population analyses.

[43] K. Kambe, *J. Phys. Soc. Jpn.* **1950**, *5*, 48–51.

[44] a) J. J. Borrás-Almenar, J. M. Clemente-Juan, E. Coronado B. S. Tsukerblat, *Inorg. Chem.* **1999**, *38*, 6081–6088; b) J. J. Borrás-Almenar, J. M. Clemente-Juan, E. Coronado, B. S. Tsukerblat, *J. Comput. Chem.* **2001**, *22*, 985–991.

[45] a) K. Eichkorn, O. Treutler, H. Öhm, M. Häser, R. Ahlrichs, *Chem. Phys. Lett.* **1995**, *242*, 652–660; b) K. Eichkorn, F. Weigend, O. Treutler, R. Ahlrichs, *Theor. Chim. Acta* **1997**, *97*, 119–124.

[46] a) A. D. Becke, *Phys. Rev. A* **1988**, *38*, 3098–3109; b) S. H. Vosko, L. Wilk, M. Nusair, *Can. J. Phys.* **1980**, *58*, 1200–1205; c) J. P. Perdew, *Phys. Rev. B* **1986**, *33*, 8822–8837.

[47] M. Dolg, H. Stoll, A. Savin, H. Preuss, *Theor. Chim. Acta*, **1989**, *75*, 173–194.

[48] *Theory and Applications of Molecular Paramagnetism* (Eds.: E. A. Boudreaux, L. N. Mulay), Wiley, New York, **1976**.

Received: September 19, 2003
Revised: June 15, 2004
Published online: September 9, 2004

